Scientific Research and Essays Vol. 6(20), pp. 4330-4340, 19 September, 2011
Available online at http://www.academicjournals.org/SRE
DOI: 10.5897/SRE11.992
ISSN 1992-2248 ©2011 Academic Journals

Full Length Research Paper

3D model retrieval approach by using fuzzy shape distributions

Kuan-Sheng Zou[1,2]*, Wai-Hung Ip[2], Chun-Ho Wu[2], Ching-Yuen Chan[2], Kai-Leung Yung[2] and Zeng-Qiang Chen[1]

[1]Department of Automation, Nankai University, Tianjin, China.
[2]Department of Industrial and Systems Engineering, the Hong Kong Polytechnic University, Hong Kong.

Accepted 24 August, 2011

With the development of graphic accelerated hardware and 3D modeling tools, 3D models will be as prevalent as other multimedia data in the future. Thus, effective content-based 3D model retrieval systems are required for emerging needs. Many 3D model retrieval methods have been proposed in recent years. Shape distributions showed superiority over others due to rotation invariance and ease of computation, but the discriminative accuracy is limited for any loss in information. Fuzzy Shape Distributions (FSD) is proposed to improve the retrieval performance of distribution-based methods. First, two improved shape distributions are presented by using the concentric partition and symmetrical partition for 3D models. Second, the two enhanced descriptors are combined with a fuzzy weighted procedure. Experimental results show that the proposed FSD can achieve better retrieval performance.

Key words: 3D model retrieval, fuzzy weighted, shape distribution, sequential quadratic programming, content-based.

INTRODUCTION

With the development of computer graphics and virtual reality, 3D models are projected to be as prevalent as other multimedia data in the future. 3D models play an important role in several domains such as computer-aided design and protein classification. Thus, there is an urgent need for an effective content based 3D model retrieval system. The key challenge to a content-based 3D model retrieval system is the extraction of the most representative features of 3D models (Tangelder and Veltkamp, 2004). The commonly adopted descriptors are global features, local features, histograms, topological features, 2D image features or combinations of the aforementioned. Bustos et al. (2007) surveyed techniques for searching for similar content in 3D object databases and a comparative study of different 3D model retrieval methods was published (Bustos et al., 2004). Iyer et al. (2005) classified and compared various 3D shape searching techniques based on shape representations and indicated directions for further research. The performance of the existing algorithms is mainly limited due to two major issues: the degeneracy of 3D objects and the variance of the description when the object is rotated, since other types of Euclidean motion such as translation and scaling normalization can be easily resolved. Concerning the rotational invariance description, two widely acceptable solutions have been applied. One is the rotational normalization of 3D models prior to feature extraction. The existing rotational normalization methods, such as continuous principle component analysis (PCA), and normal PCA (Vranic, 2003), usually improve the discriminative power of the descriptors, but some similar models cannot easily be normalized using the same coordinates (Papadakis et al., 2007).

The other method makes use of a native rotation invariant 3D model description, such as a D2 descriptor (Osada et al., 2002), spherical harmonics descriptor (SHD) (Kazhdan et al., 2003), light field descriptor (LFD) (Chen et al., 2003) and shells (Ankerst et al., 1999). A shell descriptor is easy to compute but results in low retrieval performance. The SHD and LFD can produce better results, but they are not so robust against the degeneracy of 3D objects. In contrast, a D2 descriptor which is a probability distribution histogram of two randomly selected points from the object's surface is robust against a 3D object's degeneracy. However, it

*Corresponding author. E-mail: zoukuansheng@163.com.

sacrifices discriminative accuracy. A modified D2 descriptor was proposed (Ip et al., 2002) in which each D2 histogram is classified into three types: in distance, mixed distance, and out distance. The assignment of these distances depends on whether the line segment connecting the two points lies completely inside, partially inside or completely outside an object. However, the classification of these three cases is a hard task. The angle-distance (AD) and absolute angle-distance (AAD) descriptors were proposed to compare 3D models (Ohbuchi et al., 2005). AAD measures the distribution of absolute angles between the normal vectors of two associated surfaces where the randomly selected points are located and is then combined with the distance of two selected points. It is a two dimensional descriptor which contains both the distance and the angle information. An exhaustive study of second order 3D shape features was carried out, and many combined shape descriptors were proposed based on group integration such as beta/distance (BD) and alpha/beta/distance (ABD). Experiments showed that further improvements of shape distributions can also lead to better results than the well-known methods (Reisert et al., 2006). Principal plane analysis was used for 3D model retrieval (Chen and Cheng, 2007). A principal plane is a distinctive characteristic of 3D models and finding more principal planes is useful for representing more information about 3D models. Combining different descriptors is also a hot topic in recent years.

A widely used approach is based on fixed weights assigned to each descriptor (Atmosukarto et al., 2005; Ohbuchi and Hata, 2006). The retrieval performance can be improved but many experiments are needed. Two improved ABD descriptors are proposed in this paper based on the two model-partitioning methods; they are concentric circle partition based on spatial distribution and symmetrical partition based on principal plane analysis. Statistical ABD histograms are applied to different parts to express more position information on the sample points on the surface of 3D models and then the two enhanced shape distributions are combined with a fuzzy weighted procedure in order to automatically regulate the weights of each descriptor in the retrieval process. This leads to high discriminative power. The rest of the paper is organized as follows: Subsequently, after an overview of the related 3D model work, the two improved shape distributions are described after which the fuzzy weighted procedure is explained. This is followed by the study's experimental results; finally, the study is concluded.

RELATED WORK

Principal plane analysis

In the case of 3D feature space S^3, the principal plane H can be represented as Equation 16:

$$Ax + By + Cz = D \quad (1)$$

The origin of the 3D space is translated to the centroid of the 3D model and D becomes zero. A, B and C are the directional normal vectors of H that satisfy the following relationship:

$$A^2 + B^2 + C^2 = 1 \quad (2)$$

The principal plane is the plane H with the minimal value of $\delta(S^3, H)$:

$$J = \min \delta(S^3, H) = \sum_{(x,y,z)\in S^3} \sum (Ax+By+Cz)^2 \quad (3)$$

Differentiate J with respect to A, B, C and then set to zero gives:

$$\begin{cases} m_{2,0,0}A + m_{0,1,1}B + m_{1,0,1}C = 0 \\ m_{1,1,0}A + m_{0,2,0}B + m_{0,1,1}C = 0 \\ m_{1,1,0}A + m_{0,2,0}B + m_{0,1,1}C = 0 \end{cases} \quad (4)$$

$m_{s,t,u}$ is a 3D moment given by:

$$m_{s,t,u} = \sum_{(x,y,z)\in S^3} \sum x^s y^t z^u \quad (5)$$

From Equations 4 and 5, it can be seen that:

$$\frac{A}{B} = \frac{m_{0,2,0}m_{1,0,1} - m_{1,1,0}m_{0,1,1}}{m_{2,0,0}m_{0,1,1} - m_{1,1,0}m_{1,0,1}} = k_1 \quad (6)$$

$$\frac{C}{B} = \frac{m_{0,2,0}m_{1,0,1} - m_{0,1,1}m_{1,1,0}}{m_{0,0,2}m_{1,1,0} - m_{0,1,1}m_{1,0,1}} = k_2 \quad (7)$$

Combine Equations 2, 6 and 7, and the normal vector (A, B, C,) of H is obtained.

$$(A,B,C) = \left(\frac{k_1}{\sqrt{1+k_1^2+k_2^2}}, \frac{1}{\sqrt{1+k_1^2+k_2^2}}, \frac{k_2}{\sqrt{1+k_1^2+k_2^2}} \right) \quad (8)$$

Thus, the principal plane of the 3D model is obtained, whose normal vector is n_{p1} = (A, B, C). The principal plane is considered as the first symmetrical plane in this research.

ABD descriptor

BD and ABD descriptors are proposed when the shape distribution is embedded in the theory of group integration

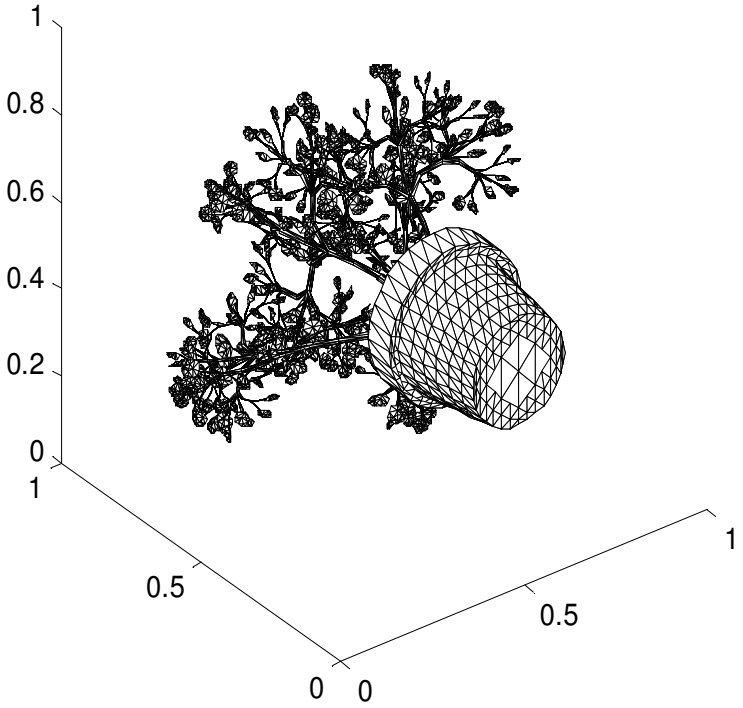

Figure 1. A 3D model.

(Reisert and Burkhardt, 2006). The feature extraction process of 3D models can be briefly explained as follows: random points are sampled using the Monte Carlo sampling model (Osada et al., 2002), then the distance of two points, the angles of two associated surface normal vectors and the angle of the distance vector with one of the surface normal vectors are measured. Finally their probability distributions are computed and the ABD histogram obtained. The ABD histogram combines all three attributes: the distance, the angles between the surface normal vectors, and the angles between the distance vector and one of the surface normal vectors in a three dimensional histogram. It is defined by:

$$ABD(d,\alpha,\beta)=\int_{(p_1,p_2)\in S\times S}\delta_d\left(\|p_1-p_2\|\right)\delta_\alpha\left(|n_1\cdot n_2|\right)\delta_\beta\left(\frac{|n_1\cdot(p_1-p_2)|}{\|p_1-p_2\|}\right) \quad (9)$$

The dimensions of distance, alpha and beta angles of ABD histogram are set as 16, 4 and 4 respectively.

MATERIALS AND METHODS

The steps for the two improved ABD descriptors are listed as follows: first, a 3D surface is randomly sampled using the Monte Carlo sampling method (Osada et al., 2002). A 3D model is shown in Figure 1, where its sampled representation is shown in Figure 2. It can be seen that the 3D surface can be randomly sampled using the Monte Carlo sampling model. A model-partitioning method is proposed to improve the ABD descriptor in which a statistical ABD histogram is used in different parts of the 3D models in order to combine more local information with the ABD descriptor. There are two model-partitioning methods; concentric circle partitioning based on the distance from the model surface to the center and symmetric partitioning based on principal plane analysis (Chen and Cheng, 2007).

Concentric ABD

The center of 3D model m_p is calculated by Equation 10.

$$m_p=\frac{\sum_{i=1}^{N} tp_i\times S_i}{S} \quad (10)$$

Where S is the total surface area, tp_i is the center of the triangle and S_i is the area of the triangle. For example, a model is divided into two parts by two concentric circles. Firstly, N random points are obtained by the Monte Carlo sampling method (Osada et al., 2002); the farthest distance between the points to the center R is calculated, then the radius of the two concentric circles are set as $0.5*R$ and R respectively. Thus the model is partitioned into two parts which are the internal part and the external part. There are three types for the two selected random points: both in the internal part (type I), both in the external part (type III) and in the different parts (type II) as shown in Figure 3.

All three types of ABD histograms are calculated and the dimensions of distance, alpha angle and beta angle of each type are set as 8, 4 and 4 respectively. A concentric/alpha/beta/distance (CABD) histogram consists of all these three types of concentric partitioned ABD histograms combined together which is described

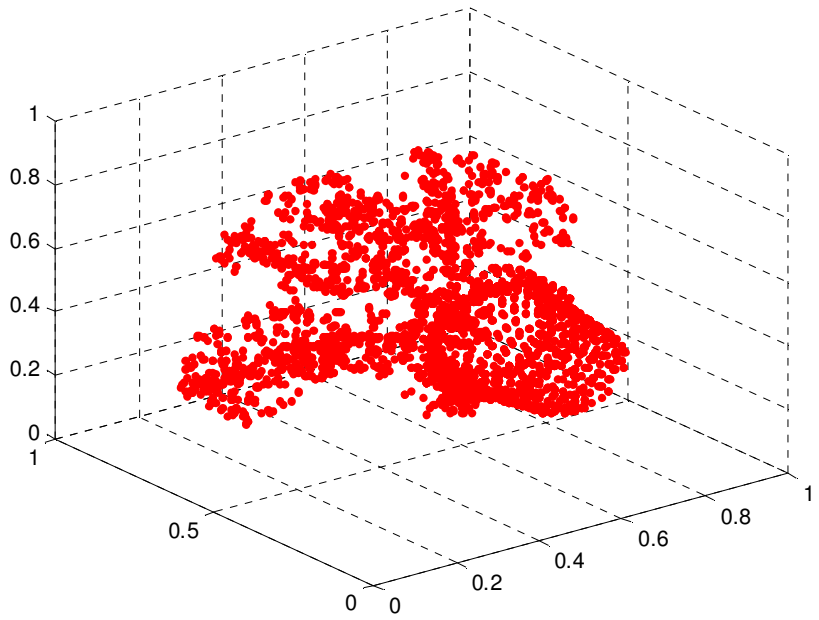

Figure 2. The sampled representation of a 3D model.

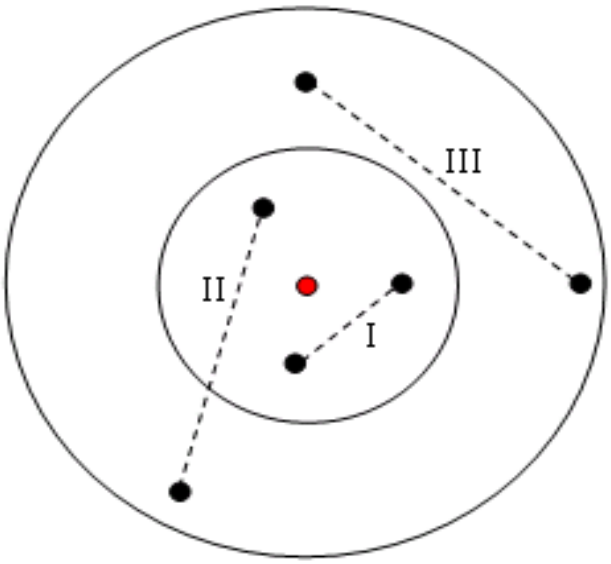

Figure 3. Concentric partitioning for the randomly sampled points; type I: the two selected points both in the internal part; type II: the two selected points in the different parts; type III: the two selected points both in the external part.

as follows:

$CABD = (CABD_I, CABD_{II}, CABD_{III})$.

Symmetrical ABD

It is noted that $n_{p2} = (A_2, B_2, C_2)$, which is the normal vector of the second symmetrical plane. The problem regarding the second principal plane should be satisfied by the following conditions: it is perpendicular to the first symmetrical plane and points on the 3D model's surface have the least distance to the second symmetrical plane. Hence, the problem of solving the second symmetrical plane can be transformed into the following constrained quadratic programming:

$$f = \min\left\{m_{200}x_1^2 + m_{020}x_2^2 + m_{002}x_3^2 + 2m_{110}x_1x_2 + 2m_{101}x_1x_3 + 2m_{011}x_2x_3\right\} \quad (11)$$

$$s.t \quad \begin{cases} A_1x_1 + B_1x_2 + C_1x_3 = 0 \\ x_1^2 + x_2^2 + x_3^2 = 1 \end{cases} \quad (12)$$

The objective function, which is shown in Equation 11 is deduced by combing Equations 3 and 5. The constraint condition which is given in Equation 12 is obtained by geometry. Solving the optimal objective function with constraints is calculated by sequential quadratic programming (Boggs and Tolle, 1995), giving $n_{p2} = (A_2, B_2, C_2) = (x_1, x_2, x_3)$.

The 3D model is partitioned into four symmetrical parts by the two symmetrical planes. There are three different types of the two random points: in the same symmetrical part (type I), in the adjacent parts (type II) and in the diagonal parts as shown in Figure 4. All the three types of ABD histograms are calculated. The dimensions of distance, alpha angle and beta angle of each type are set as 8, 4 and 4 respectively. A symmetrical/alpha/beta/distance (SABD) histogram consists of these three types of symmetrical partitioned ABD histograms combined together and is represented as follows:

$SABD = (SABD_I, SAB_{II}, SABD_{III})$.

Fuzzy weighted procedure

When combining the two improved descriptors, the weights should

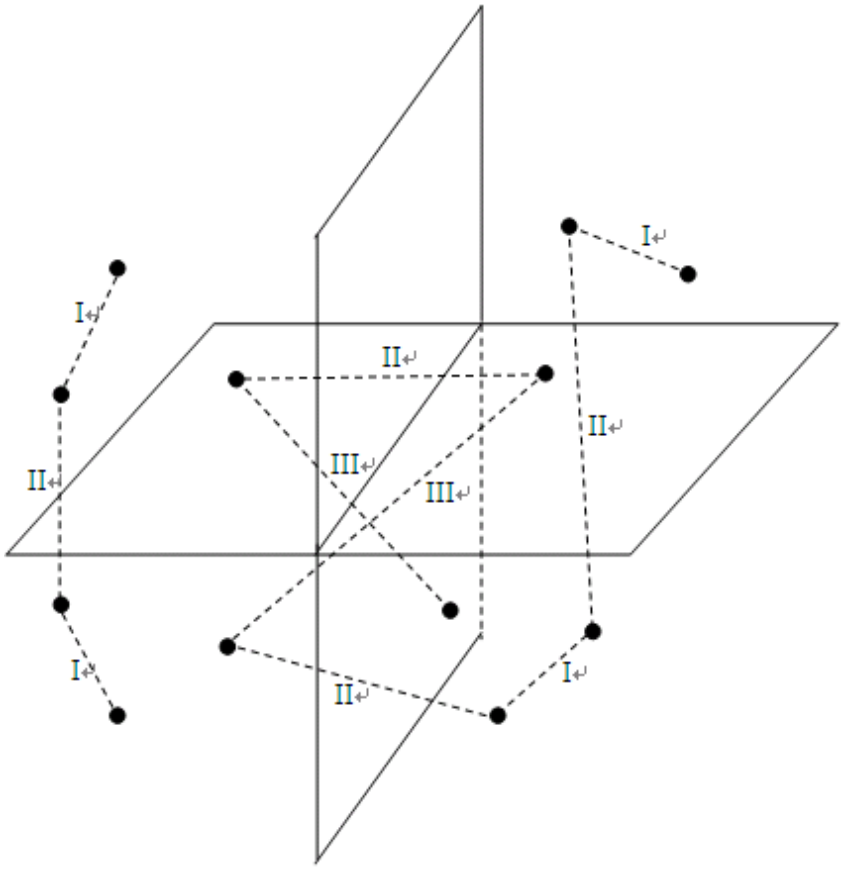

Figure 4. Symmetrical partition for the randomly sampled points; type I: the two selected points both in the same symmetrical part; type II: the two selected points in the adjacent parts; type III: the two selected points both in the diagonal parts.

be adjusted dynamically according to their performance. Fuzzy weighted procedure is thus introduced. Firstly, the query model is selected, and then the CABD and SABD descriptors are extracted. The CABD and SABD descriptors of the query model are compared with the feature database and the distance between the query model and the searched model is calculated. For example, let *a*, *b* be two 3D models. h_a and h_b are in the two histograms (CABD or SABD). The distance of the CABD and SABD can be calculated in the Equations 11 and 12.

$$d_{CABD}=\sum_{i=1}^{N_d}\sum_{j=1}^{N_\alpha}\sum_{k=1}^{N_\beta}\frac{2\left|h_{CABDa}(i,j,k)-h_{CABDb}(i,j,k)\right|}{\left|h_{CABDa}(i,j,k)+h_{CABDb}(i,j,k)\right|} \quad (13)$$

$$d_{SABD}=\sum_{i=1}^{N_d}\sum_{j=1}^{N_\alpha}\sum_{k=1}^{N_\beta}\frac{2\left|h_{SABDa}(i,j,k)-h_{SABDb}(i,j,k)\right|}{\left|h_{SABDa}(i,j,k)+h_{SABDb}(i,j,k)\right|} \quad (14)$$

The final similarity of the fuzzy shape distributions (FSD) is defined as Equation 13.

$$d_{FSD}=W_a\times d_{CABD}+W_b\times d_{SABD} \quad (15)$$

Where $W_a + W_b = 1$.

The value of W_a is decided by using a fuzzy logic method. The nearest neighbor (NN) and first-tier (FT) are the two important measures of the retrieval performance. They are introduced as the feedback input values to adjust the weights W_a and W_b. NN is the percentage in which the closest match belongs to the same class as the query model and *FT* is the percentage of models which belongs to the query class that appears within the *C*-1 matches, where *C* is the number of 3D models in one category. If the *NN* or *FT* value of CABD is larger, it means that the CABD descriptor has a better retrieval performance than the SABD descriptor, so the weight of the CABD, W_a, should be adjusted to a bigger value in order to obtain better results. Since it only requires searching the top *C*-1 closest models using the CABD and the SABD descriptors respectively, it does not introduce a computational burden to the retrieval process.

Firstly, the *NN* and *FT* of *Da* and *Db* are calculated, and the two fuzzy input values: *In1* and *In2* are obtained from Equation 14.

$$In1=\frac{NN1}{NN1+NN2},\quad In2=\frac{FT1}{FT1+FT2} \quad (16)$$

The membership functions of the input value: *In1* and *In2* are shown in Figure 5a, while the membership of the output value is shown in Figure 5b. When the percentage of *NN* or *FT* of one retrieval method increases, experiment results show that one particular retrieval method is better than the other one, so the

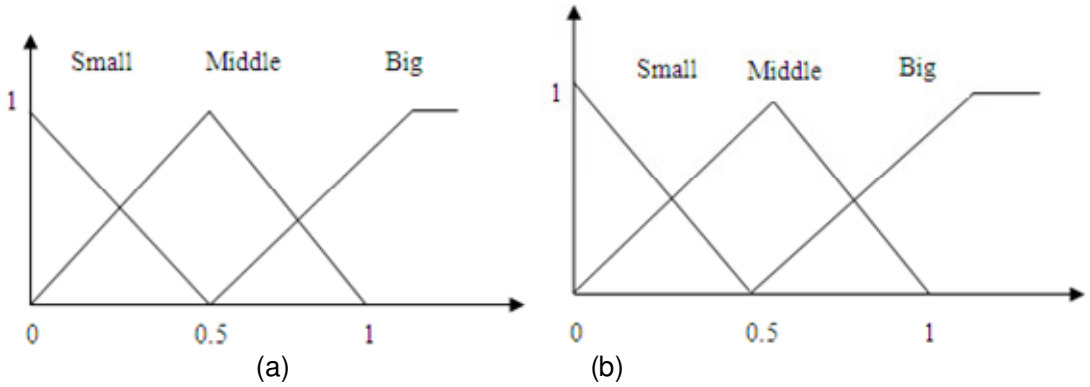

Figure 5. The membership function of the input (a) and the output value (b).

weight of this method should be bigger. Accordingly, the fuzzy rules are defined as follows:

If In_1 is small and In_2 is small, W_a is *big*.
If In_1 is small and In_2 is middle, W_a is middle.
If In_1 is small and In_2 is big, W_a is middle.
If In_1 is middle and In_2 is small, W_a is middle.
If In_1 is middle and In_2 is middle, W_a is middle.
If In_1 is middle and In_2 is big, W_a is small.
If In_1 is big and In_2 is small, W_a is middle.
If In_1 is big and In_2 is middle, W_a is middle.
If In_1 is big and In_2 is big, W_a is small.

The output values of W_a are solved by the weighted average method, thus W_b can be obtained by $W_b = 1-W_a$, finally obtaining the similarity of the FSD.

RESULTS AND DISCUSSION

The database of the Princeton shape benchmark (PSB) is used in the experiment (Shilane et al., 2004). The PSB provides a set of 1814 classified 3D models which are divided into 907 training and 907 testing models. 500 models from each of these two groups are selected. The training models are classified into 20 categories and each category contains 25 models. The testing models are classified into 25 categories and each category has 20 models. The PC test platform is Intel Core 2 Quad, 3 GHZ CPU, 2 G RAM with Windows XP professional operating system. The precision-recall diagram and the other four quality measures in the following are used for performance evaluation.

Recall and precision-recall plot

For each query model in class *C* and any number *K* of top matches, 'recall' is the percentage of models in class *C* accurately retrieved within the top *K* matches. The recall *(R)* in this research is computed when $K = 5C$. Precision (*P*) represents the percentage of the top *K* matches which are members of class *C*, and the precision-recall plot indicates the relationship between precision and recall in a ranked list of matches. Curves closer to the upper right corner represent superior retrieval performance.

Nearest neighbor (NN)

The percentage of models that are closest to the query and which are in the same category.

First-tier (FT) and second-tier (ST)

They are the percentage of models belonging to the same category as the query that appears within the top (*C*-1) and 2* (*C*-1) matches respectively.

E-measure (EM)

This is a composite measure of the precision and recall for the first 32 retrieved models which is defined by:

$$EM = \frac{2*P*R}{P+R} \tag{17}$$

The average retrieval performance evaluation is done in such a way that each 3D model in the dataset is used as a query model to search for other similar models for testing. Thus, the average evaluation is obtained. Taking recall values of descriptors in the test dataset as an example: the average recall is calculated by:

$$recall = \frac{1}{500}\sum_{i=1}^{20}\sum_{j=1}^{25} recall_i^j \tag{18}$$

Where $recall_i^j$ represents the recall value when the j-th model in the category is selected as the query model.

Table 1. Retrieval performance of descriptors on the training dataset.

Descriptors	NN (%)	FT (%)	ST (%)	EM (%)	R (%)
Shells	19.8	16.4	23.3	16.5	39.9
D2	35.4	22.6	33.1	23.2	54.2
Moments	55.2	30.9	41.9	30.2	57.9
AAD	49.8	30.9	43.2	30.7	63.0
ABD	59.0	33.6	46.6	33.4	67.5
CABD	63.4	37.2	52.0	36.9	79.9
SABD	66.2	36.7	48.9	35.5	65.6
FSD	70.8	39.9	54.5	38.9	82.1

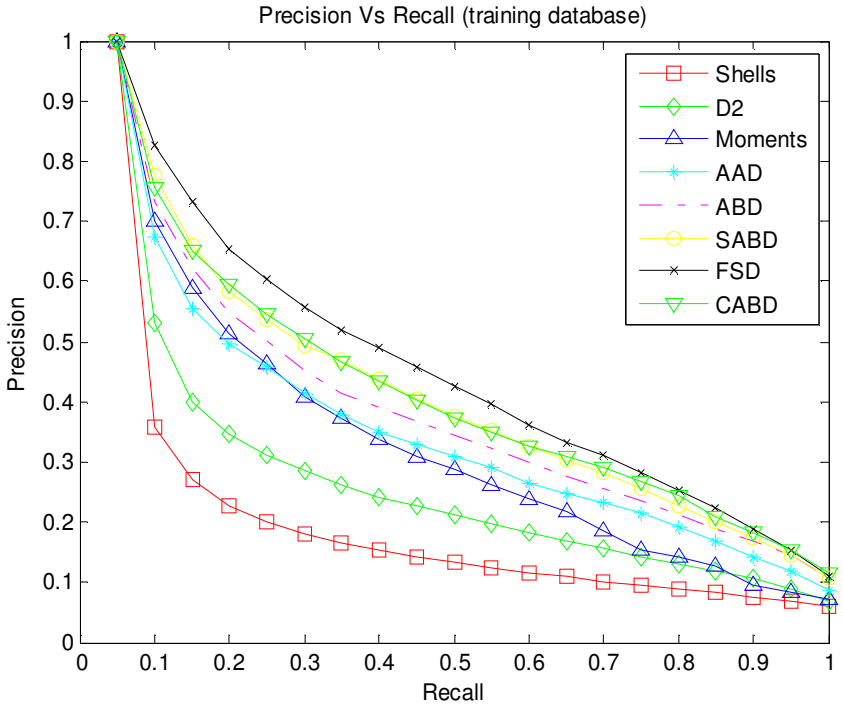

Figure 6. The precision-recall curves of the training database.

The retrieval performances of the descriptors using the training dataset are shown in Table 1. In general, the proposed CABD and SABD descriptors are better than the ABD in Table 1. The proposed FSD method has the best retrieval performance and has improved performance, especially in *NN* and *R* values. The precision-recall curves of the testing dataset are shown in Figure 6. It is obvious that FSD is greatly improved compared to the others, while the retrieval performance of CABD and SABD are similar to each other, but both of them are better than the ABD descriptor.

The retrieval performances of the descriptors of the testing dataset are shown in Table 2. Compared with D2, the *NN*, *FT*, *ST*, *EM* and *R* values of FSD are improved respectively by 125.6, 82.2, 59.5, 74.1 and 47.63% respectively. Obviously, the *NN* value is highly improved by using the proposed FSD. Since *NN* value measures the accuracy of searching the most similar models, FSD performs much better than other descriptors, thus, the proposed FSD has further potential to be applied in the practice. The precision-recall curves of descriptors for the testing dataset are shown in Figure 7, while the performance measures are shown in Table 2. It can be seen that, in the testing dataset, the proposed FSD performs better than it is in the training dataset. The CABD and SABD also achieve better results than the ABD descriptor. In comparing the FSD method with other well-known methods, the experiment is also carried out on the base-level classification of PSB, which is a test dataset containing 907 3D models. All the reference

Table 2. Retrieval performance of descriptors on the testing dataset.

Descriptors	NN (%)	FT (%)	ST (%)	EM (%)	R (%)
Shells	22.8	17.9	26.7	18.5	47.0
D2	36.0	24.1	36.5	25.1	59.0
Moments	57.8	30.9	42.3	31.0	58.7
AAD	56.8	32.6	46.2	33.5	66.9
ABD	61.4	34.9	49.9	35.8	72.3
CABD	65.8	38.7	53.8	39.3	81.0
SABD	66.8	37.6	50.8	37.9	69.8
FSD	81.2	43.9	58.2	43.7	87.1

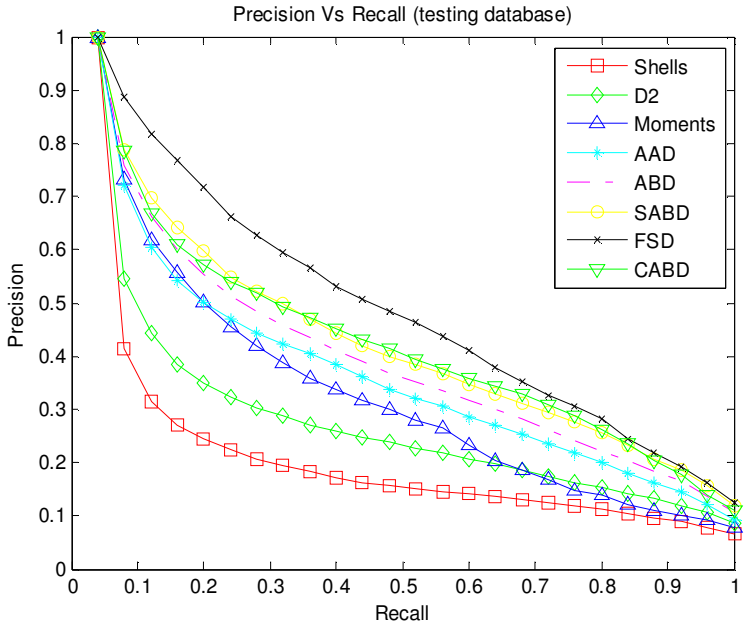

Figure 7. The precision-recall curves of the testing database.

results in Table 3 can be found in previous published work (Reisert and Burkhardt, 2006; Shilane et al., 2004). The other three methods included are used for comparison.

Spherical harmonics of GEDT (SH-GEDT)

This is a rotation invariant representation of the GEDT obtained by computing the restriction of the function to concentric spheres and storing the norm of each frequency (Kazhdan et al., 2003).

Gaussian Euclidean distance transform (GEDT)

This is based on the comparison of a 3D function whose value at each point is obtained by combining a Gaussian with a Euclidean distance transform of the surface (Kazhdan et al., 2003).

Adaptive views clustering (AVC)

It provides an optimal selection of 2-D views from a 3D model and a probabilistic Bayesian method for 3D model retrieval from these views. The characteristic view selection algorithm is based on an adaptive clustering algorithm and uses statistical model distribution scores to select the optimal number of views (Ansary et al., 2007).

It can be seen that the CABD and the SABD have similar performances to the SHD and GEDT shown in Table 3, while FSD is better than all of them. The *NN* and *EM* values of FSD are better than that of AVC, Although FSD has smaller values in *FT* and *ST* than LFD, the size of

Table 3. Comparison to the best known methods on the entire PSB dataset.

Descriptors	NN (%)	FT (%)	ST (%)	EM (%)	Size
D2	34.2	16.9	25.2	15.2	32
ABD	54.7	27.4	37.5	22.5	256
GEDT	60.3	31.3	40.7	23.7	16384
SHD	55.6	30.9	41.1	24.1	1092
AVC	60.6	33.2	44.3	25.5	1113
CABD	60.8	29.7	40.1	23.8	384
SABD	56.9	28.7	38.6	23.2	384
FSD	68.3	32.9	43.4	26.1	768

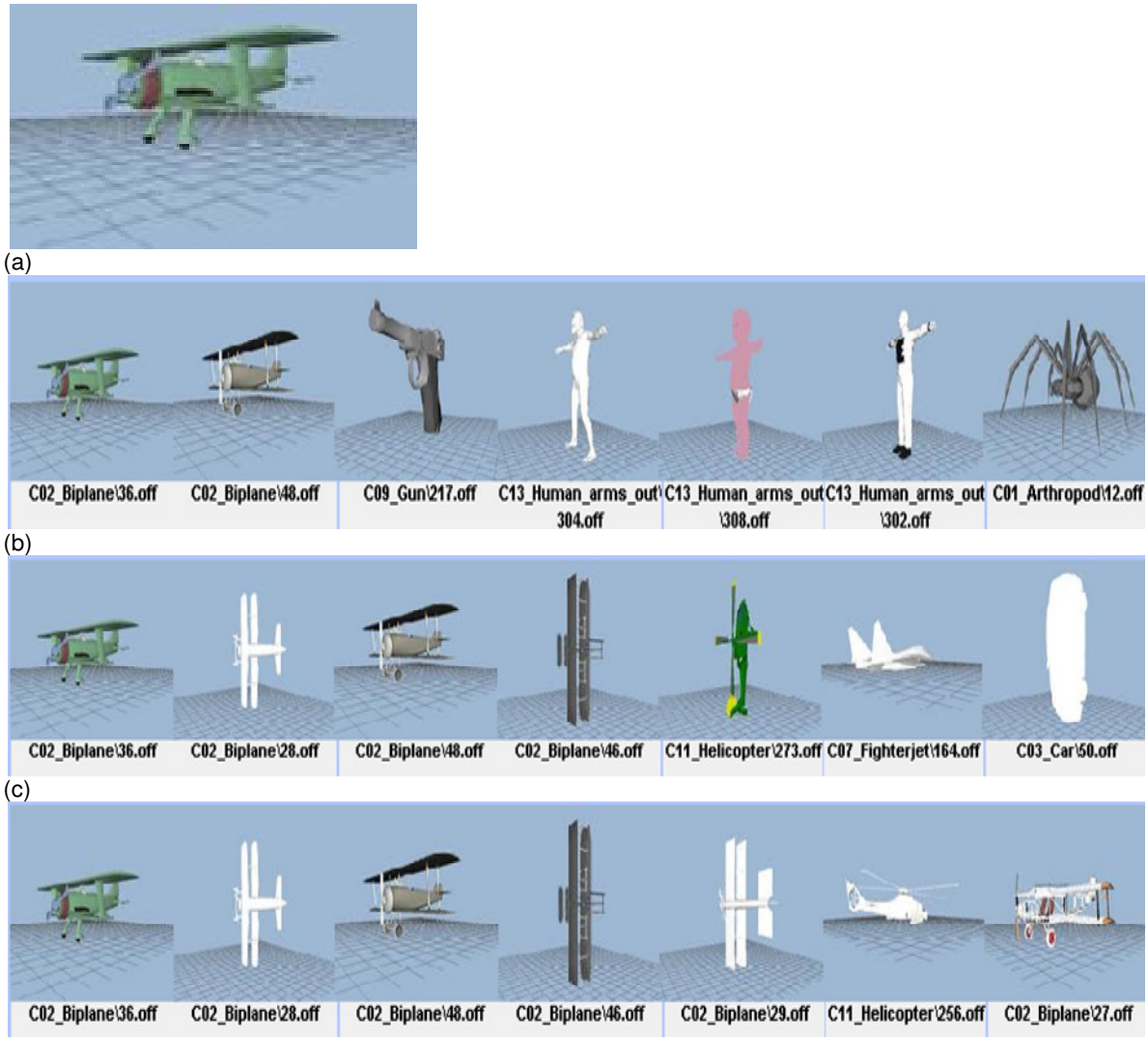

Figure 8. Visual retrieval results for 'Biplane' category. (a) Query model; (b) D2; (c) ABD; and (d) FSD.

LFD is bigger than FSD and AVC needs expensive computational time. The visual retrieval results using the proposed FSD, compared with D2 and ABD are shown in Figures 8 and 9. Figure 8a is a query model selected in the 'Biplane' category. The retrieval results using D2, ABD and FSD are shown in Figures 8b, c and d

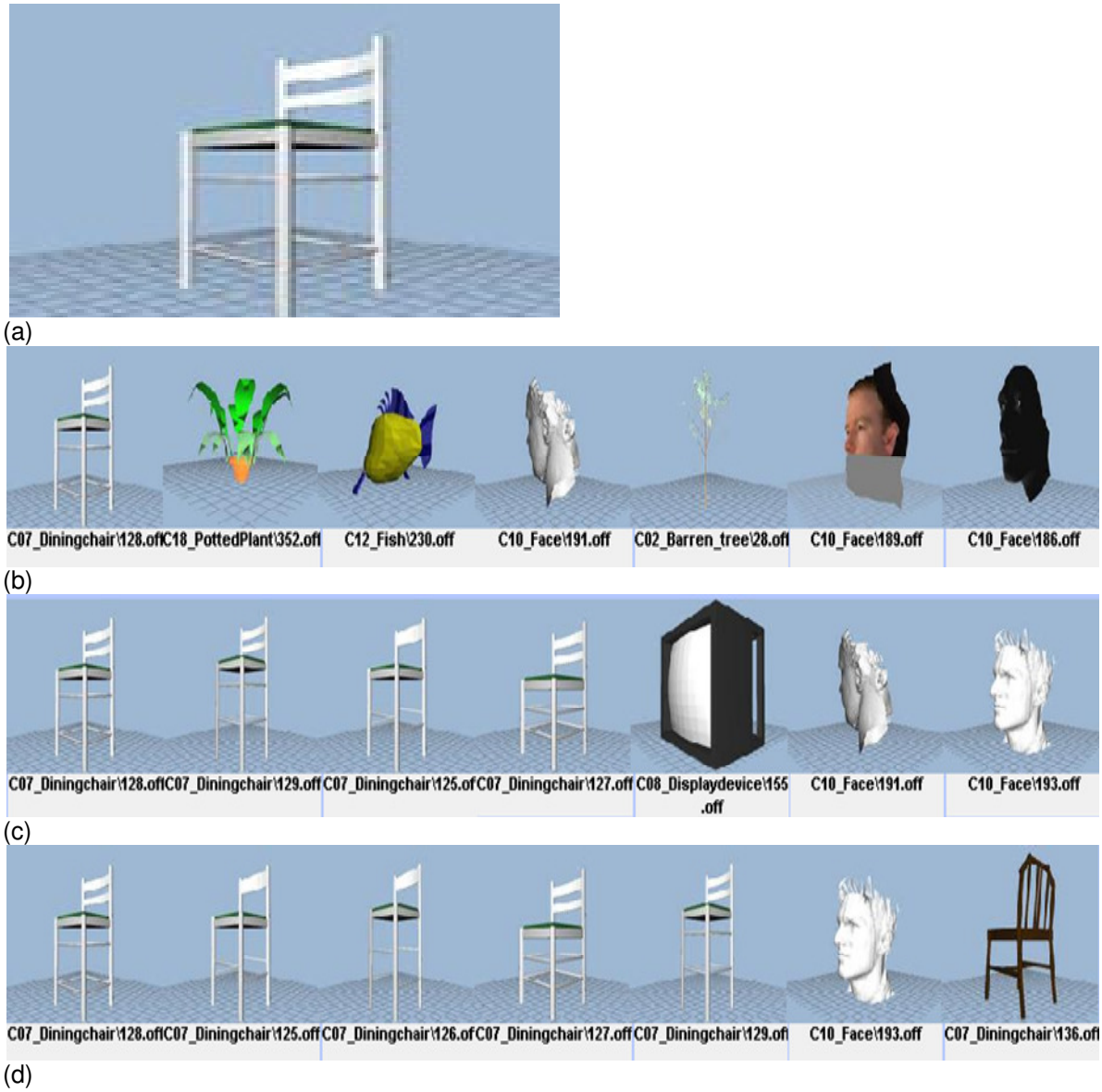

Figure 9. Visual retrieval results for 'Dining chair' category. (a) Query model; (b) D2; (c) ABD; and (d) FSD.

respectively. Only 2 related models are retrieved in the top 7 by D2 and 4 models are retrieved by ABD while 6 models are retrieved by using the proposed FSD. Obviously, the retrieval performance using FSD is improved by 200 and 50% compared with D2 and ABD respectively. Figure 9a is a query model selected in the 'Diningchair' category. The retrieval results using D2, ABD and FSD are shown in Figures 9b, 9c and 9d respectively. Only 1 model is retrieved in the top 7 by D2 and 4 models are retrieved by ABD, while 6 models are retrieved using the proposed FSD.

The retrieval performance by using FSD is improved by 500 and 50% compared with D2 and ABD respectively. It is obvious that the proposed FSD can obtain much better retrieval results than D2 and ABD greatly in practice.

Conclusion

The fuzzy shape distribution (FSD) is proposed for 3D model retrieval. First, the concentric ABD (CABD) and symmetrical ABD (SABD) are introduced to improve the ABD descriptor because they can exploit more location information of random points on the surface of 3D models. Secondly, FSD is presented by combining CABD and SABD with a fuzzy weighted procedure. Experimental results show that the proposed methods obtain a very good retrieval performance. Due to the

good characteristic and performance of the shape distribution based method, further work is needed to extract more meaningful and distinctive characteristics of 3D models to improve the retrieval results. Furthermore, this fuzzy weighted procedure can be also extended to other combinations of retrieval methods. Its main advantage is that it only needs to compute the top *C* nearest models and adjust the weights according to the searching performance of these models.

ACKNOWLEDGEMENTS

Our gratitude is extended to the research committee and the Department of Industrial and System Engineering of the Hong Kong Polytechnic University for support in this project (G-U726). This work was also supported in part by the Natural Science Foundation of China Under Grants of 61174094 and 60904064, the Specialized Research Fund for the Doctoral Program of Higher Education of China Under Grant 20090031110029.

REFERENCES

Ankerst M, Kastenmuller G, Kriegel H, Seidl T (1999). 3D Shape Histograms for Similarity Search and Classification in Spatial Database, Advances in Spatial Databases: 6th Int. Sym., Washington, DC, USA, pp. 207-226.

Ansary TF, Daoudi M, Vandeborre JP (2007). A Bayesian 3-D Search Engine Using Adaptive Views Clustering. IEEE Trans. Multimedia., 9 (1): 78-88.

Atmosukarto I, Leow WK, Huang ZY (2005). Feature Combination and Relevance Feedback for 3D Model Retrieval. Proc. 11th Int. Multimedia Modeling Conf., Melbourne, Australia, pp. 334-339.

Boggs PT, Tolle JW (1995), Sequential Quadratic Programming. Acta Numerica, 4:1-51.

Bustos B, Keim D, Saupe D, Schreck T (2007). Content-based 3D Object Retrieval. IEEE Comput. Graph., 27: 22-27.

Bustos B, Keim D, Saupe D, Schreck T, Vranic D (2004). An Experimental Comparison of Feature-based 3D Retrieval Methods. Visualization and Transmission: 2th Int. Sym. 3D Data Proc., Thessaloniki, Greece, pp. 215-222.

Chen DY, Tian XP, Shen YT, Ouhyoung M (2003). On Visual Similarity based 3D Model Retrieval. Comput. Graph. Forum., 22: 223-232.

Chen TK, Cheng, SC (2007). 3D Model Retrieval Using Principle Plane Analysis and Dynamic Programming. Pattern Recogn., 40:742-755.

Ip CY, Lapadat D, Sieger L, Regli WC (2002). Using Shape Distributions to Compare Solid Models. 7th ACM Sym. Solid Modeling and Appl., Saarbrücken, Germany, pp. 273-280.

Iyer N, Jayanti S, Lou K, Kalyanaraman Y, Ramani K (2005). Three-dimensional Shape Searching: State-of-the-art Review and Future Trends. J. Comput Aid Des., 37: 509-530.

Kazhdan M, Funkhouser T, Rusinkiewicz S (2003). Rotation Invariant Spherical Harmonic Representation of 3D Shape Descriptors. Sym. Geom. Proc., Vienna, Austria, pp. 156-164.

Ohbuchi R, hata Y (2006).Combining Multiresolution Shape Descriptors for Effective 3D Similarity Search, Proc. WSCG 2006, Plzen, Czech Republic.

Ohbuchi R, Minamitani T, Takei T (2005). Shape-similarity Search of 3D Models by Using Enhanced Shape Functions. Int. J. Comput. Appl. Technol., 23: 70-85.

Osada R, Funkhouser T, Chazelle B, Dobkin D (2002). Shape Distributions, ACM Trans. Graph, 21: 807-832.

Papadakis P, Pratikakis I, Perantonis S, Theoharis T, (2007): Efficient 3D Shape Matching and Retrieval Using A Concrete Radicalized Spherical Projection Representation. Pattern Recog., 40: 2437-2452.

Reisert M, Burkhardt H (2006). Second Order 3D Shape Features: An Exhaustive Study. Comput. Graph., 30: 197-206.

Shilane P, Min P, Kazhdan M, Funkhouser T (2004). The Princeton Shape Benchmark. Shape Modeling Int., Genova, Italy, pp.167-178.

Tangelder JWH, Veltkamp RC (2004). A Survey of Content Based 3D Shape Retrieval Methods, Shape Modeling Int., Genova, Italy, pp. 145-156.

Vranic DV (2003). An Improvement of Rotation Invariant 3D-Shape based on Functions on Concentric Spheres. Int. Conf. Image Processing, Barcelona, Spain, pp. 757-760.